Theoretical investigation on the electronic structure, elastic properties, and intrinsic hardness of Si_2N_2O

Ding Ying-Chun(丁迎春)†, Chen Min(陈 敏),
Gao Xiu-Ying(高秀英), and Jiang Meng-Heng(蒋孟衡)

College of Optoelectronics Technology, Chengdu University of Information Technology, Chengdu 610225, *China*

(Received 8 September 2011; revised manuscript received 7 December 2011)

According to the density functional theory we systematically study the electronic structure, the mechanical properties and the intrinsic hardness of Si_2N_2O polymorphs using the first-principles method. The elastic constants of four Si_2N_2O structures are obtained using the stress-strain method. The mechanical moduli (bulk modulus, Young's modulus, and shear modulus) are evaluated using the Voigt–Reuss–Hill approach. It is found that the tetragonal Si_2N_2O exhibits a larger mechanical modulus than the other phases. Some empirical methods are used to calculate the Vickers hardnesses of the Si_2N_2O structures. We further estimate the Vickers hardnesses of the four Si_2N_2O crystal structures, suggesting all Si_2N_2O phases are not the superhard compounds. The results imply that the tetragonal Si_2N_2O is the hardest phase. The hardness of tetragonal Si_2N_2O is 31.52 GPa which is close to values of β-Si_3N_4 and γ-Si_3N_4.

Keywords: elastic property, Vickers hardness, electronic structure

PACS: 71.15.Mb, 71.20.–b, 62.20.–x, 62.20.Qp **DOI:** 10.1088/1674-1056/21/6/067101

1. Introduction

Compounds in the Si–O–N system exhibit good thermal, chemical, and mechanical stabilities, as well as adjustable diffusion barriers and dielectric properties.[1] One such phase is stoichiometric silicon oxynitride named Si_2N_2O, a refractory material with all the aforementioned desirable properties. Recently, Si_2N_2O has been intensively studied because of its better dielectric performance than SiO_2- and Si_3N_4-based devices.[2,3] Moreover, silicon oxynitride (Si_2N_2O) is also a unique compound in the SiO_2–Si_3N_4 quasi-binary system, and can be considered as a link between the two important engineering materials, i.e. Si_3N_4 and SiO_2.[4] Like Si_3N_4, Si_2N_2O is an engineering material and can keep excellent oxidation resistance in air at temperatures up to 1600 °C, and high flexural strength at temperatures up to 1400 °C without significant degradation.[5,6] The structure and the compressibility of sinoite Si_2N_2O have been studied in detail. The sinoite (Si_2N_2O) structure is built from SiN_3O tetrahedral linked with puckered hexagonal Si_2N_2 layers through O atoms.[7–11] The reason that Si_2N_2O has not been widely used recently is its very wide band gap (5.20 eV). Crudely speaking, sinoite is an insulator. On the other hand, it is not as hard as α-Si_3N_4 or β-Si_3N_4, so it has limited mechanical applications. In addition, Si_2N_2O is considered a promising candidate for electro-optics and organic light-emitting devices,[12,13] i.e., Si_2N_2O has been proposed for use in integrated optical communication devices.[14] The ground state properties of orthorhombic Si_2N_2O ($Cmc2_1$) have been reported in previous studies, i.e. the electronic structure, stability, elasticity, and optical properties.[15–18] Recently theoretical simulations and experiments on the phase stability of sinoite Si_2N_2O predict a series of phase transformations.[19–21] Kroll and Milko[19] studied the phase transitions of Si_2N_2O polymorphs using density functional theory calculations. They investigated two dense phases of Si_2N_2O, i.e., a defect spinel structure at a moderate pressure and a corundum-type structure at very high pressure. The decomposition and the amorphization of Si_2N_2O are also reported. Sekine *et al.*[20] found the partial amorphization of sinoite at about 34 GPa, and there was no phase transition in their experiment. Liu *et al.*[22] studied the ground state, elastic stiffness and dielectric constants of orthorhombic Si_2N_2O with various native point defects. Zhang *et al.*[23] calculated the electronic structure, the elastic constants, and the optical properties of orthorhombic Si_2N_2O according to the density-functional theory through the Cambridge Sequential Total Energy Package (CASTEP), using the local den-

†Corresponding author. E-mail: dyccqzx@yahoocom.cn

© 2012 Chinese Physical Society and IOP Publishing Ltd

sity approximation (LDA), with ultra-soft pseudopotential (USPP).

In the present paper, we further study the electronic structures, the elastic properties, and the Vickers hardnesses of the four Si_2N_2O (orthorhombic Si_2N_2O, β-In_2S_3-type, alternative spinel-like, and α-Al_2O_3-type Si_2N_2O) structures using first principles calculations.

2. Calculation methods and models

Density functional theory (DFT) has played an important role. This *ab-initio* approach is applied at various levels and has been shown to lead to some significant results regarding the prediction of structural, elastic, and thermodynamic properties.[24−28] The first principles calculations based on DFT were conducted in CASTEP code with PBE for solids (PBEsol).[29] The plane wave basis set was used for the energy calculations. For plane wave expansion in reciprocal space, the kinetic energy cutoff was set at 350 eV. The frozen core approximation was used for the pseudo-atoms. The ultra-soft pseudopotential (USPP) of the Vanderbilt scheme was used to account for the electrostatic interaction between valence electrons and the ionic core.[30] For elements Si, N, and O, the valence electron configurations are $2s^23p^2$ (Si), $2s^22p^3$ (N), and $2s^22p^4$ (O), respectively. The energy integrations were performed on a discretized k grid in the first irreducible Brillouin zone, and we used 10×10×10, 4×4×5, 5×5×2, 6×6×3 k point meshes for the four Si_2N_2O polymorphs. The method proposed by Monkhorst–Pack was used to generate the k points in this paper. The Pulay density mixing scheme is applied to the electronic energy minimization. For the convergence, the change of total energy was set at 1×10^{-6} eV/cell; the mean Hellmann–Feymann force acting on the atom was reduced to 0.01 eV/Å (1 Å=0.1 nm).

At ambient conditions Si_2N_2O has an orthorhombic structure with a space group $Cmc2_1$ (NO. 36). The unit cell of orthorhombic Si_2N_2O contains 20 atoms. There are at least two different views. The first one considers hexagonal Si_2N_2-layers stacked on top of each other. These layers are puckered and connected via O atoms, which complete the tetrahedron around the Si atoms. Half of the Si atoms are linked to the layer above and the other half to the layer below. Nitrogen atoms are approximately trigonal-planar coordinated, and the Si–O–Si bond angle is bent. Kroll *et al.*[19] studied hypothetical high-pressure modifications of Si_2N_2O with three different structures. The β-In_2S_3-type has a spinel-like structure. S atoms are approximately set in tetrahedral siting (16h) in a cubic-closed packing. However, a third of all tetrahedral sites typically filled in the spinel structure are vacant. The ordering of vacancies causes the atoms to be appreciably displaced and the symmetry to reduce from $Fd\bar{3}m$, the space group of the ideal spinel, to $I4_1/amd$. The unit cell of β-In_2S_3-type contains 80 atoms. Kroll and Milko[19] probed different substitution patterns and found a monoclinic polymorph with space group symmetry $C2/m$. The unit cell of alternative spinel-like Si_2N_2O contains 80 atoms. The

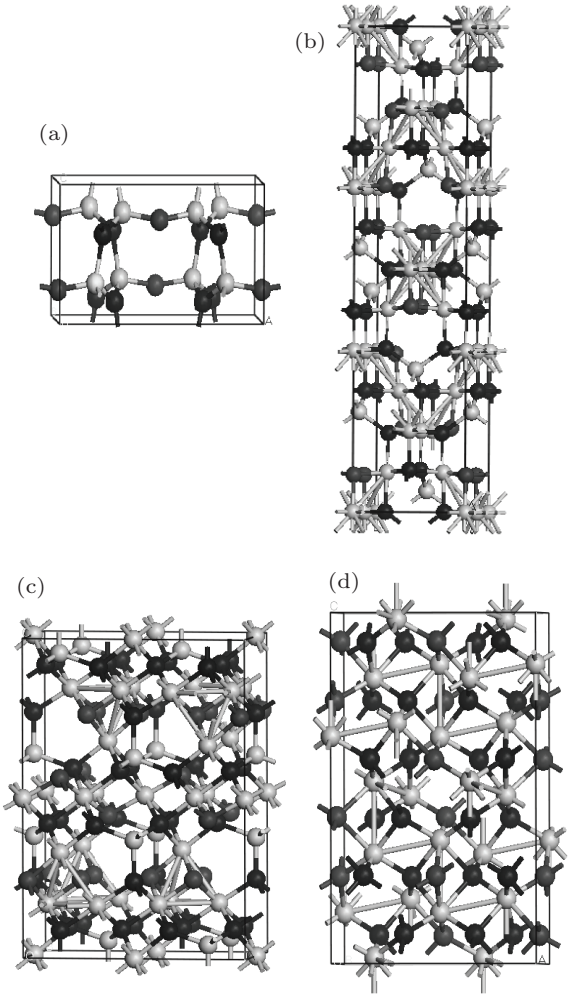


Fig. 1. Crystal structures of Si_2N_2O polymorphs. The light gray atoms denote silicon atoms, the black atoms represent nitrogen atoms, and the light black atoms refer to oxygen atoms. Panel (a) is for orthorhombic Si_2N_2O ($Cmc2_1$, No. 36, $Z = 4$), panel (b) for β-In_2S_3-type Si_2N_2O (tetragonal system, $I4_1/amd$, No. 141, $Z = 16$), panel (c) for alternative spinel-like Si_2N_2O (monoclinic system $C2/m$, No. 12 $Z = 16$), and panel (d) for α-Al_2O_3-type Si_2N_2O (monoclinic system $C2/c$, No. 15, $Z = 12$).

corundum (α-Al_2O_3) is the most stable polymorph of Al_2O_3 under ambient conditions. The arrangement of anions is close to a hexagonal-closed-packing. The mapping of Si_2N_2O onto the corundum structure leads to a symmetry reduction. The α-Al_2O_3-type Si_2N_2O takes a monoclinic structure with a space group with $C2/c$. The unit cell of α-Al_2O_3-type Si_2N_2O contains 60 atoms.

The four crystal structures of orthorhombic ($Cmc2_1$, No. 36), tetragonal (β-In_2S_3-type, $I4_1/amd$, No. 141), and two monoclinic (spinel type, $C2/m$, No. 12; α-Al_2O_3-type, $C2/c$, No. 15) Si_2N_2O polymorphs are shown in Fig. 1. The details about the lattice constants and atomic positions can be found in Ref. [19]. From the experiments, orthorhombic Si_2N_2O is the ground state at low pressure and temperature. The three other crystal structures of Si_2N_2O are merely theoretical predictions at present, and there is no clear evidence to confirm or deny the existence of these high pressure phases.

3. Results and discussion

3.1. Electronic structures

The densities of state (DOSs) and partial densities of states (PDOSs) of the four polymorphs of Si_2N_2O are shown in Fig. 2. The total density of state (TDOS) and partial density of states (PDOS) of orthorhombic Si_2N_2O ($Cmc2_1$, No. 36) are shown in Fig. 2(a). The DOS features are consistant with those reported by other researchers.[22,23,31] As can be seen the conduction band is mostly derived from Si 2p electron states. While the N 2p electrons dominate the top of the valence band, a mixture of O 2p and Si sp electron states in the valence band (-10 eV to 0 eV) is also significant. Si electron states are located in the conduction band (> 5 eV). N 2p electron states reside at the top of the valence band (-10 eV to 0 eV) and significantly N 2s electron states stay in the valence band (-17 eV to -13 eV). O 2p electron states are at the top of the valence band (-10 eV to 0 eV) and O 2s electron states apparently exist in the valence band (-20 eV to -18 eV). The DOS near the Fermi level is dominated by 2p bands of N atoms. The strong hybridizations with the 2p orbital of N and 2p orbital of O can be clearly seen in Fig. 2(a). The contributions from the 2s and 2p orbital of Si atoms are relatively small but not negligible. From these results, we conclude that the main orbital interactions in orthorhombic Si_2N_2O are due to 2p (N)–2p (O).

By analysing the PDOS, it is found that the N 2p states have some admixtures with the O 2p and Si sp states. Thus, the orthorhombic Si_2N_2O ($Cmc21$, No. 36) structure appears to have some covalent features.

The electronic structures of the other three structures (β-In_2S_3-type Si_2N_2O, alternative spinel-like Si_2N_2O, α-Al_2O_3-type Si_2N_2O) have not been calculated in other papers. For β-In_2S_3-type Si_2N_2O (Fig. 2(b)), the conduction bands originate mainly from the contributions of the 2s and 2p orbitals of Si and the 2p orbitals of N atoms. The O atoms slightly contribute to the conduction bands. The bottom of valence bands between -22.0 eV and -17.5 eV are from 2s orbitals of O atoms. The valence bands between -17.5 eV and -12.5 eV come from 2p orbitals of N atoms. The highest occupied valence band (the top of the valence band) consists of Si sp electron states, N 2p orbitals and O 2p orbitals. The electronic DOSs near the Fermi surface are mainly from the contributions of O 2p orbitals. The covalent features originate mainly from 2p orbitals of Si and 2p orbitals of N atoms. Therefore, we can conclude that β-In_2S_3-type Si_2N_2O also has some covalent features.

For the alternative spinel-like Si_2N_2O (Fig. 2(c)), the conduction bands originate mainly from the contribution of the 2s and 2p orbitals of Si and the little 2p orbitals of N atoms, the O atoms make no contribution to the conduction bands. The bottom of valence bands between -21.0 eV and -17.5 eV are from 2s orbitals of O atoms. The valence bands between -17.5 eV and -12.5 eV are from the 2p orbitals of N atoms. The major contribution of VBs between -10 eV and 0 eV is mainly from Si sp electron states, N 2p orbitals and O 2p orbitals. The electronic density near the Fermi surface is mainly from the contribution of the N 2p and O 2p orbitals. The covalent features originate mainly from 2p orbitals of N and 2p orbitals of O atoms.

The conduction bands and top valence bands of α-Al_2O_3-type Si_2N_2O (Fig. 2(d)) and the alternative spinel-like Si_2N_2O (Fig. 2(c)) in DOS are similar. The bottom valence bands between -21.0 eV and -18 eV derive from the 2s orbitals of O atoms. The valence bands between -17.5 eV and -12.5 eV are from the 2p orbitals of N atoms.

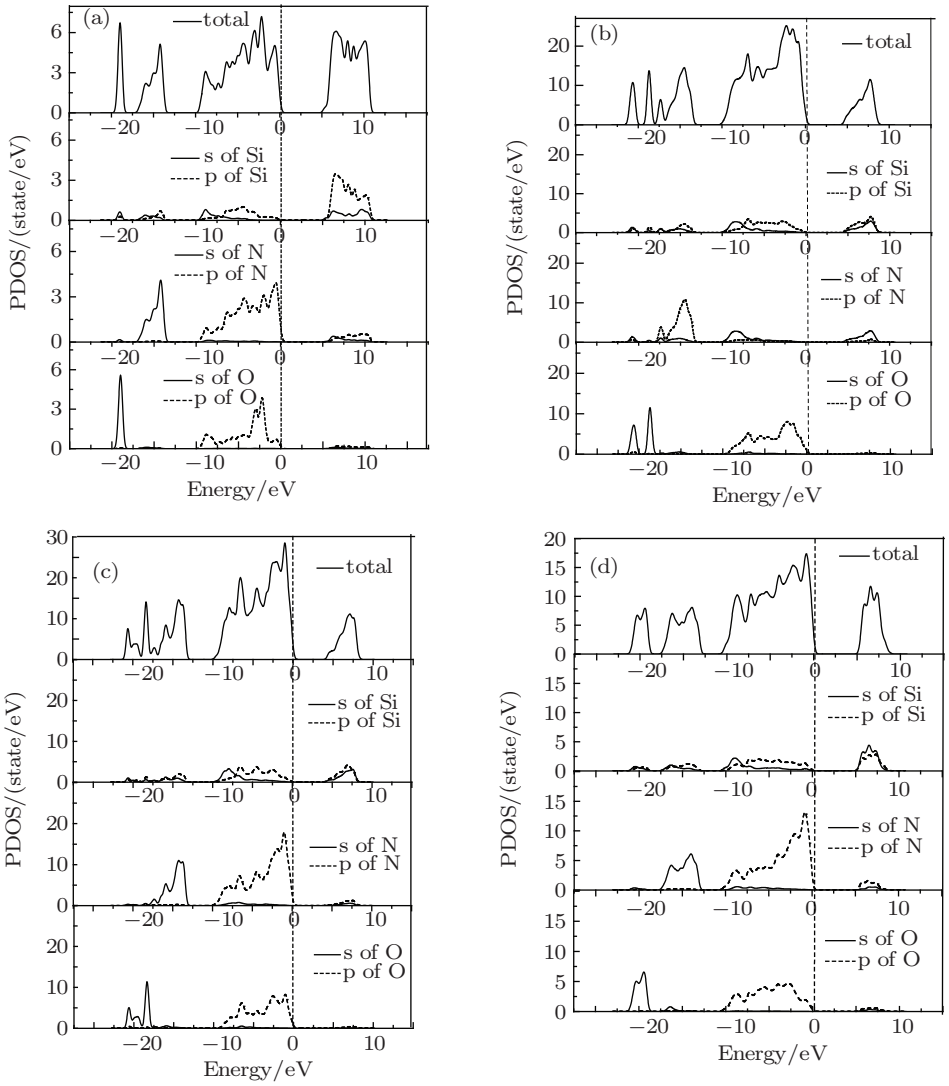


Fig. 2. (colour online) Total densities of state (TDOSs) and partial densities of states (PDOSs) of four Si_2N_2O polymorphs: (a) orthorhombic Si_2N_2O ($Cmc2_1$), (b) β-In_2S_3-type Si_2N_2O ($I4_1/amd$), (c) alternative spinel-like Si_2N_2O ($C2/m$), (d) α-Al_2O_3-type Si_2N_2O($C2/c$).

3.2. Mechanical properties

The calculated Si_2N_2O compounds in this work belong to three crystal classes, orthorhombic, tetragonal, and monoclinic, respectively. For orthorhombic Si_2N_2O, we compare our results with other theoretical calculations. Only the independent elastic constants are listed for each crystal structure. In the following section, we will introduce the formulas of elastic moduli and mechanical stability criteria for the considered crystal systems.[32–34]

Orthorhombic phase (C_{11}, C_{22}, C_{33}, C_{44}, C_{55}, C_{66}, C_{12}, C_{13}, and C_{23})

$$B_{\mathrm{V}} = \frac{1}{9}(C_{11}+C_{22}+C_{33}) + \frac{2}{9}(C_{12}+C_{13}+C_{23}), \quad (1)$$

$$G_{\mathrm{V}} = \frac{1}{15}(C_{11}+C_{22}+C_{33}) - \frac{1}{15}(C_{12}+C_{13}+C_{23}) + \frac{1}{5}(C_{44}+C_{55}+C_{66}), \quad (2)$$

$$B_{\mathrm{R}} = \frac{1}{(S_{11}+S_{22}+S_{33})+2(S_{12}+S_{13}+S_{23})}, \quad (3)$$

$$G_{\mathrm{R}} = \frac{15}{4(S_{11}+S_{22}+S_{33})-4(S_{12}+S_{13}+S_{23})+3(S_{44}+S_{55}+S_{66})}. \quad (4)$$

The mechanical stability criteria are given by

$$
\begin{aligned}
&C_{11}>0,\ \ C_{22}>0,\ \ C_{33}>0,\\
&C_{44}>0,\ \ C_{55}>0,\ \ C_{66}>0,\\
&[C_{11}+C_{22}+C_{33}+2\,(C_{12}+C_{13}+C_{23})]>0,\\
&(C_{11}+C_{22}-2C_{12})>0,\\
&(C_{11}+C_{33}-2C_{13})>0,\\
&(C_{22}+C_{33}-2C_{23})>0. \qquad (5)
\end{aligned}
$$

Tetragonal phase (C_{11}, C_{33}, C_{44}, C_{66}, C_{12}, and C_{13})

$$
\begin{aligned}
B_{\rm V} &= \frac{1}{9}\left[2\,(C_{11}+C_{12})+C_{33}+4C_{13}\right], \qquad (6)\\
G_{\rm V} &= \frac{1}{30}\left(M+3C_{11}-3C_{12}+12C_{44}+C_{66}\right), \qquad (7)\\
B_{\rm R} &= C^2/M, \qquad (8)
\end{aligned}
$$

$$
\begin{aligned}
&G_{\rm R}=\frac{15}{(18B_{\rm V}/C^2)+[6/(C_{11}-C_{12})]+(6/C_{44})+(3/C_{66})}, \qquad (9)\\
&M=C_{11}+C_{12}+2C_{33}-4C_{13},\quad C^2=(C_{11}+C_{12})\,C_{33}-2C_{13}^2.
\end{aligned}
$$

The mechanical stability criteria are given by

$$
\begin{aligned}
&C_{11}>0, C_{33}>0, C_{44}>0, C_{66}>0,\\
&(C_{11}-C_{12})>0,\\
&(C_{11}+C_{33}-2C_{13})>0,\\
&(2\,(C_{11}+C_{12})+C_{33}+4C_{13})>0. \qquad (10)
\end{aligned}
$$

Monoclinic phase (C_{11}, C_{22}, C_{33}, C_{44}, C_{55}, C_{66}, C_{12}, C_{13}, C_{23}, C_{15}, C_{25}, C_{35}, and C_{46})

$$
\begin{aligned}
B_{\rm V} &= \frac{1}{9}\,(C_{11}+C_{22}+C_{33})\\
&\quad+\frac{2}{9}\,(C_{12}+C_{13}+C_{23}), \qquad (11)\\
G_{\rm V} &= \frac{1}{15}\,(C_{11}+C_{22}+C_{33})-\frac{1}{15}\,(C_{12}+C_{13}+C_{23})\\
&\quad+\frac{1}{5}\,(C_{44}+C_{55}+C_{66}), \qquad (12)\\
B_{\rm R} &= \Omega[a\,(C_{11}+C_{22}-C_{12})+b\,(2C_{12}-2C_{11}-C_{23})\\
&\quad+c\,(C_{15}-2C_{25})\\
&\quad+d\,(2C_{12}+2C_{23}-C_{13}-2C_{22})\\
&\quad+2e\,(C_{25}-C_{15})+f]^{-1}, \qquad (13)\\
G_{\rm R} &= 15\{4[a\,(C_{11}+C_{22}+C_{12})+b\,(C_{11}-C_{12}-C_{23})\\
&\quad+c\,(C_{15}+C_{25})+d\,(C_{22}-C_{12}-C_{23}-C_{13})\\
&\quad+e\,(C_{15}-C_{25})+f]/\Omega\\
&\quad+3\left[g/\Omega+(C_{44}+C_{66})/\left(C_{44}C_{66}-C_{46}^2\right)\right]\}^{-1}, \qquad (14)
\end{aligned}
$$

$$
\begin{aligned}
&a=C_{33}C_{55}-C_{35}^2,\quad b=C_{23}C_{55}-C_{25}C_{35},\\
&c=C_{13}C_{35}-C_{15}C_{33},\quad d=C_{13}C_{55}-C_{15}C_{35},\\
&e=C_{13}C_{25}-C_{15}C_{23},\\
&f=C_{11}\left(C_{22}C_{55}-C_{25}^2\right)-C_{12}\,(C_{12}C_{55}-C_{15}C_{25})\\
&\quad+C_{15}\,(C_{12}C_{25}-C_{15}C_{22})\\
&\quad+C_{25}\,(C_{23}C_{35}-C_{25}C_{33}),\\
&g=C_{11}C_{22}C_{33}-C_{11}C_{23}^2-C_{22}C_{13}^2\\
&\quad-C_{33}C_{12}^2+2C_{12}C_{13}C_{23},\\
&\Omega=2[C_{15}C_{25}\,(C_{33}C_{12}-C_{13}C_{23})\\
&\quad+C_{15}C_{35}\,(C_{22}C_{13}-C_{12}C_{23})\\
&\quad+C_{25}C_{35}\,(C_{11}C_{23}-C_{12}C_{13})\\
&\quad-C_{15}^2\left(C_{22}C_{33}-C_{23}^2\right)+C_{25}^2\left(C_{11}C_{33}-C_{13}^2\right)\\
&\quad+C_{35}^2\left(C_{11}C_{22}-C_{12}^2\right)+gC_{55}.
\end{aligned}
$$

The mechanical stability criteria are given by

$$
\begin{aligned}
&C_{11}>0, C_{22}>0, C_{33}>0, C_{44}>0, C_{55}>0, C_{66}>0,\\
&[C_{11}+C_{22}+C_{33}+2\,(C_{12}+C_{13}+C_{23})]>0,\\
&\left(C_{11}C_{55}-C_{12}^2\right)>0,\quad \left(C_{44}C_{66}-C_{46}^2\right)>0,\\
&(C_{22}+C_{33}-2C_{23})>0; \qquad (15)\\
&[C_{22}\left(C_{33}C_{55}-C_{35}^2\right)+2C_{23}C_{25}C_{35}\\
&-C_{23}^2C_{55}-C_{25}^2C_{33}]>0, \qquad (16)\\
&2[C_{15}C_{25}\,(C_{33}C_{12}-C_{13}C_{23})\\
&+C_{15}C_{35}\,(C_{22}C_{13}-C_{12}C_{23})\\
&+C_{25}C_{35}\,(C_{11}C_{23}-C_{12}C_{13})]-[C_{15}^2\left(C_{22}C_{33}-C_{23}^2\right)\\
&+C_{25}^2\left(C_{11}C_{33}-C_{13}^2\right)+C_{35}^2\left(C_{11}C_{22}-C_{12}^2\right)\\
&+C_{55}(C_{11}C_{22}C_{33}-C_{11}C_{23}^2-C_{22}C_{13}^2\\
&-C_{33}C_{12}^2+C_{12}C_{13}C_{23}]>0. \qquad (17)
\end{aligned}
$$

The obtained elastic constants of the four Si_2N_2O structures satisfy the conditions for stability. As a result, the crystal structures of Si_2N_2O polymorphs are stable. From the calculated elastic constants, we can see that the mechanical strength along the [010] direction is weaker than along the other two directions for orthorhombic Si_2N_2O, i.e. the [100] and [001] directions. The obtained C_{11} (326 GPa) and C_{33} (324 GPa) values of this phase are close to each other, and are slightly larger than C_{22} (302 GPa). Haines and Santoro[21] reported on the linear compressibility of orthorhombic Si_2N_2O using the X-ray diffraction method for the three main axes, i.e., $k_{\rm a}$, $k_{\rm b}$, and $k_{\rm c}$ in

[100], [010], and [001] directions, respectively. They found that $k_a \approx k_c < k_b$, strong evidence showing that $C_{11} \approx C_{33}$. We also compare our results with other theoretical calculations. C_{11} and C_{33} values are smaller than those values obtained by another calculation in the LDA. However, PBEsol predicts a smaller C_{22} value than the LDA, and the reason has not been clear so far. A force field investigation of orthorhombic Si_2N_2O in Ref. [22] also provided accurate C_{ij} values comparable to first principles calculations. Our PBEsol results are in agreement with the force field calculations. Zhang *et al.*[23] also calculated the elastic constants of orthorhombic Si_2N_2O using the LDA in CASTEP code. Their values are actually consistant with those in Ref. [22]. Although the LDA underestimates the lattice constants, most elastic constants obtained by this function are larger than PBEsol values except for C_{22}. For C_{11}, C_{22}, and C_{33} of orthorhombic Si_2N_2O the present results indicate that the mechanical moduli are more isotropic in the (010) crystal plane than in the (100) plane and the (001) plane. In Ref. [15], the full set of elastic constants of orthorhombic Si_2N_2O were also obtained by a molecular dynamical simulation method. However, the values reported in Ref. [15] are quite different from those in other references and this paper, for instance, C_{23} is 5 GPa which is too small. On the other hand, C_{44}, C_{55}, and C_{66} represent the shear moduli in (100), (010), and (001) crystal planes, respectively. For the orthorhombic Si_2N_2O, we find that C_{44} is greatly larger than C_{55} and C_{66}, but C_{66} is close to C_{55}. Therefore, the shear modulus will show strong directional independence. Finally, C_{12}, C_{13}, and C_{23} are the mechanical moduli which correspond to biaxial strain (stress), i.e., shear moduli of (110) plane along $[1\bar{1}0]$ direction ((110) $[1\bar{1}0]$), ((101) [101]), and ((011) [011]) , respectively. The non-central symmetric forces among the atoms in the crystal structures can be characterized by the difference between the pure shear and biaxial moduli, i.e., the difference between C_{44} and C_{12}. For the other three Si_2N_2O polymorphs, they all have larger C_{ij} values than the orthorhombic Si_2N_2O. The largest C_{11} value is observed for tetragonal Si_2N_2O, and it is 603 GPa. In addition, for tetragonal Si_2N_2O, we can observe $C_{11} = C_{22}$, $C_{44} = C_{55}$, and $C_{13} = C_{23}$ which are larger than the values of the orthorhombic phase. The C_{12} of tetragonal Si_2N_2O is the smallest one of all the Si_2N_2O structures, which may deteriorate the mechanical moduli of this phase. For the two monoclinic Si_2N_2O phases, the obtained elastic constants are slightly different from each other, especially for the non-diagonal tensor elements, i.e. C_{23}, C_{15}, C_{25}, and C_{35}. The negative tensor elements are obtained for the two monoclinic structures; however, the values of C_{15}, C_{25}, C_{35}, and C_{46} are smaller than the diagonal tensor elements. As a result, we can also use Eq. (5) for the orthorhombic structure, to measure the mechanical stability of monoclinic crystal class.

Table 1. Calculated independent elastic constants (C_{ij}) of Si_2N_2O.

		C_{ij}/GPa												
Species	Method	C_{11}	C_{22}	C_{33}	C_{44}	C_{55}	C_{66}	C_{12}	C_{13}	C_{23}	C_{15}	C_{25}	C_{35}	C_{46}
	CASTEP-PBEsol	326	302	324	131	57	71	112	72	68				
	Dynamics simulation[15]	319	165	250	99	81	90	46	33	5				
		343	220	286	108	89	98	64	61	42				
	CASTEP-LDA[22]	336	264	336	142	61	78	99	63	57				
$Cmc2_1$	CASTEP-GULP[22]	323	270	336	139	57	72	95	68	55				
	LDA/UPP[16]	316.0	241.6	320.7	139.1	59.7	76.2	81.3	51.5	31.0				
	GGA/UPP[16]	313.9	252.3	320.3	136.7	61.6	76.0	84.0	53.6	36.5				
	CASTEP-LDA[23]	330.4	278.2	329.2	135.5	62.3	75.0	104.3	66.4	51.5				
$I4_1/amd$	CASTEP-PBEsol	603		534	264		138	49	169					
$C2/m$	CASTEP-PBEsol	543	548	570	177	173	213	105	59	60	–55	53	–0.14	54
$C2/c$	CASTEP-PBEsol	579	624	645	178	152	217	181	93	94	28	–31	–2	–29

The mechanical moduli, i.e. shear modulus (G), bulk modulus (B), and Young's modulus (E) are calculated using the Voigt–Reuss–Hill approximation from the elastic constants. The VRH approximation provides the reasonable mechanical moduli for bulk polycrystalline material. The fundamental relationships are given as

$$B_H = (B_V + B_R)/2, \tag{18}$$

$$G_H = (G_V + G_R)/2, \tag{19}$$

$$E = 9B_{\rm H}G_{\rm H}/(3B_{\rm H} + G_{\rm H}), \quad (20)$$

$$\nu = (3B_{\rm H} - 2G_{\rm H})/[2\,(3B_{\rm H} + G_{\rm H})], \quad (21)$$

where the subscripts H, V, and R refer to Hill, Voigt, and Reuss approximations, respectively; ν is Poisson's ratio. Voigt and Reuss approximations provide the upper and lower bounds of mechanical moduli for a bulk polycrystalline material, respectively.

Table 2. Elastic compliance matrix (S_{ij}) of Si_2N_2O.

	S_{ij}												
Species	S_{11}	S_{22}	S_{33}	S_{44}	S_{55}	S_{66}	S_{12}	S_{13}	S_{23}	S_{15}	S_{25}	S_{35}	S_{46}
$Cmc21$	0.0036	0.0039	0.0033	0.0076	0.0174	0.0139	–0.0012	–0.0006	–0.0005				
$I41/amd$	0.0018	0.0018	0.0023	0.0038	0.0038	0.0072	0.0000	–0.0006	–0.0006				
$C2/m$	0.0020	0.0020	0.0018	0.0061	0.0063	0.0051	–0.0004	–0.0002	–0.0002	0.0008	–0.0008	0.0000	–0.0016
$C2/c$	0.0020	0.0018	0.0016	0.0058	0.0067	0.0047	–0.0006	–0.0002	–0.0002	–0.0004	0.0005	0.0000	0.0008

In the above equations, C_{ij} denotes the elastic stiffness matrix shown in Table 1, S_{ij} is the elastic compliance matrix shown in Table 2, and S_{ij} is the inverse matrix of C_{ij} and can be calculated easily. The mechanical moduli for all Si_2N_2O polymorphous obtained from the Voigt–Reuss–Hill approximation are given in Table 3. The results are also compared with other theoretical calculations available. From the results, we can observe that the bulk modulus of orthorhombic Si_2N_2O is 161.9 GPa which is significantly smaller than those of the other three Si_2N_2O structures. The calculated bulk moduli of high pressure phases of Si_2N_2O by PBEsol are 220 GPa and over. On the other hand, the orthorhombic Si_2N_2O also has the smallest shear modulus of those of the four Si_2N_2O structures. The shear modulus value ($G_{\rm H}$) is found to be 93.7 GPa by the Hill approximation. Experimentally, the shear modulus of this phase is 90 GPa which approximates the value (93.7 GPa). The calculated Young's modulus of orthorhombic Si_2N_2O is also close to the experimental value. The results indicate that our results for the mechanical moduli of Si_2N_2O polymorphs are reliable. The mechanical moduli are usually used to estimate the intrinsic hardness of the crystal structure. The shear modulus (G) and the Young's modulus (E) are considered to be correlated with hardness better than bulk modulus (B).[36] From Table 3, compared with the tetragonal and monoclinic phases, the orthorhombic Si_2N_2O is less hard. The Poisson's ratios of Si_2N_2O structures are relatively small. The values are actually close to those values of covalent-ionic crystals. Ratio B/G reflects the brittality or ductility of a material, and the critical value is near 1.75. Below this value, the material is brittle; otherwise, it is ductile. Except for orthorhombic Si_2N_2O, the B/G ratios for tetragonal and monoclinic Si_2N_2O structures are smaller than 1.75. For orthorhombic Si_2N_2O, the obtained B/G ratio is pretty close to the critical value. In regard to the high pressure phases, i.e. tetragonal Si_2N_2O and monoclinic Si_2N_2O, the coordinate numbers of Si, N, and O might be larger than the numbers in the low pressure orthorhombic Si_2N_2O structure. As a result, the ionic bonds in the high pressure phases are stronger than those in orthorhombic Si_2N_2O. Therefore, both the calculated B/G ratio and v of high pressure phases of Si_2N_2O are small.

Table 3. Calculated mechanical moduli of Si_2N_2O, including bulk moduli ($B_{\rm V}$, $B_{\rm R}$, and $B_{\rm H}$), shear moduli ($G_{\rm V}$, $G_{\rm R}$, and $G_{\rm H}$), Young's modulus (E), and Poisson's ratio (v). For the mechanical moduli, which are in units of GPa.

Species	Method	$B_{\rm V}$	$B_{\rm R}$	$G_{\rm V}$	$G_{\rm R}$	$B_{\rm H}$	$G_{\rm H}$	E	v	$B_{\rm H}/G_{\rm H}$
	this work	162.1	161.6	98.8	88.6	161.9	93.7	235.6	0.257	1.73
	expt. results[35]						93.1	221.6		
$Cmc2_1$	LDA/UPP[16]					132.7	97.1	234.2		
	GGA/UPP[16]					136.4	97.3	235.8		
	CASTEP-LDA[23]					152.3	92.4	242.4		1.65
$I4_1/amd$	this work	279.4	278.8	223.7	206.9	279.1	215.3	513.8	0.193	1.30
$C2/m$	this work	234.5	234.5	208.4	190.3	234.5	199.4	466.1	0.169	1.18
$C2/c$	this work	286.9	286.4	208.0	195.0	286.7	201.5	489.8	0.215	1.42

3.3. Intrinsic hardness

To estimate the values of microhardness ($H_{\rm v}$) of the four crystal structures of Si_2N_2O, we use the following relation[37]

$$H_{\rm v} = \frac{(1-2\nu)\,E}{6\,(1+\nu)}. \tag{22}$$

Jiang *et al.*[36] recently discussed the correlations between hardness and the mechanical moduli for many covalent crystals. The following relationships are obtained for bulk modulus, shear modulus, Young's modulus, and Vickers hardness, respectively:

$$B = 10.38H_{\rm v}, \tag{23}$$

$$G = 6.78H_{\rm v}, \tag{24}$$

$$E = 16.48H_{\rm v}. \tag{25}$$

From Eq. (22), we can also estimate the Vickers hardness of each Si_2N_2O phase and the computed values are 15.18, 44.07, 43.99, and 38.30 GPa for orthorhombic Si_2N_2O, tetragonal Si_2N_2O, spinel-type Si_2N_2O, and α-Al_2O_3-type Si_2N_2O, respectively. From Eqs. (23)–(25), the computed values are 15.60, 13.82, 14.29 GPa; 26.89, 31.76, 36.18 GPa; 22.59, 29.41, 28.28 GPa; 27.72, 29.72, 29.72 GPa for orthorhombic Si_2N_2O, tetragonal Si_2N_2O, alternative spinel-type Si_2N_2O, and α-Al_2O_3-type Si_2N_2O, respectively. We find that the computed values from the method used by Miao *et al.*'s[37] are larger than the values from the method used by Jiang *et al.*'s,[36] except for 15.60 GPa which is slightly larger than the 15.18 GPa of orthorhombic Si_2N_2O. We can see that the Vickers hardness of orthorhombic Si_2N_2O obtained by Eqs. (23)–(25) is close to the experimental value (∼ 19 GPa).

Furthermore, according to Gao *et al.*'s theory,[38] in this work the theoretical hardness of single crystal can be calculated by the following forms:

$$H_{\rm v} = \left[\prod_{\mu}^{\mu}(H_{\rm v}^{\mu})^{n^{\mu}}\right]^{1/\sum_{\mu} n^{\mu}}, \tag{26}$$

$$H_{\rm v}^{\mu} = 350(N_{\rm e}^{\mu})^{2/3}\,{\rm e}^{-1.191 f_{\rm i}^{\mu}}/(d^{\mu})^{2.5}, \tag{27}$$

where $H_{\rm v}$ is the Vickers hardness of the crystal structure; $H_{\rm v}^{\mu}$ is the hardness of a μ-type bond; n^{μ} is the total number of μ-type bonds; $N_{\rm e}^{\mu}$ refers to the valence electron density of a μ-type bond; $f_{\rm i}^{\mu}$ characterizes the ionicity of i bond and d^{μ} is the bond length of μ-type bond. $N_{\rm e}^{\mu}$ can be calculated by

$$N_{\rm e}^{\mu} = (n_{\rm e}^{\mu})/\upsilon_{\rm b}^{\mu}. \tag{28}$$

In the above equation, $n_{\rm e}^{\mu}$ is the total number of valence electrons per μ bond and $\upsilon_{\rm b}^{\mu}$ denotes the bond volume. The two parameters, i.e., $n_{\rm e}^{\mu}$ and $\upsilon_{\rm b}^{\mu}$ are calculated by

$$n_{\rm e}^{\mu} = [(Z_{\rm A}^{\mu})/N_{\rm CA} + (Z_{\rm B}^{\mu})/N_{\rm CB}], \tag{29}$$

$$\upsilon_{\rm b}^{\mu} = (d^{\mu})^3/\sum_{\nu}[(d^{\nu})^3 N_{\rm b}^{\nu}], \tag{30}$$

where $N_{\rm CA}$ and $Z_{\rm A}^{\mu}$ are the coordinate number and the number of valence electrons of A atom, respectively.

The calculated values of Vickers hardness using the Gao *et al.*'s[38] method for each Si_2N_2O structure are shown in Table 4. In Gao *et al.*'s method, the hardness values are found to be less than 32 GPa for all the Si_2N_2O polymorphs. We can clearly see that the hardness values of all the Si_2N_2O phases are much higher than those of α-quartz (SiO_2), but they are not as hard as β-Si_3N_4 nor as γ-Si_3N_4[39−43] (in Table 4). The hardness values of orthorhombic Si_2N_2O and the two monoclinic Si_2N_2O phases are close to each other, 28.9, 28.9, and 29.5 GPa, respectively. The tetragonal Si_2N_2O has the highest hardness value of 31.5 GPa, which is close to those of β-Si_3N_4 and γ-Si_3N_4[39−43] (in Table 4).

In Gao *et al.*'s method, one can calculate the hardness of each chemical bond type. From the results in Table 4, we can conclude that the high hardness of tetragonal Si_2N_2O phase is attributed mainly to the Si–N and Si–O bonds. In this structure, the Si–N bond is stronger than the Si–O bond. As a result, the Si–N bond exhibits higher hardness than the Si–O bond. For two monoclinic Si_2N_2O structures, α-Al_2O_3-type Si_2N_2O has a lower hardness than the spinel Si_2N_2O. For the spinel Si_2N_2O, the calculated hardness of the Si–N bond is larger than the hardness of α-Al_2O_3-type Si_2N_2O. Therefore, alternative spinel-like Si_2N_2O possesses slightly higher hardness than α-Al_2O_3-type Si_2N_2O.

For tetragonal Si_2N_2O and two monoclinic Si_2N_2O structures, the calculated Vickers hardness using Gao *et al.*'s method accords well with that calculated using Jiang *et al.*'s method. We can especially see that the Vickers hardness of E–$H_{\rm v}$ relationship using Jiang *et al.*'s method is more consistent than with that found using Gao *et al.*'s method.

From these calculations, we conclude that tetragonal Si_2N_2O is the hardest phase in the four Si_2N_2O structures. The Vickers hardness values of the two monoclinic Si_2N_2O phases are close to each other. Moreover, the hardness of orthorhombic Si_2N_2O is

close to that of α-SiO_2 which is not a hard compound as we expected. In previous work, Gao *et al.*[38] have calculated the Vickers hardness of α-SiO_2. The theoretical value was found to be 30 GPa, significantly larger than the experimental result, i.e. 11 GPa.[11] The large discrepancy between the two values is due mainly to the open structure of α-SiO_2. The same reason can be used to explain our results for orthorhombic Si_2N_2O. For a superhard compound, the Vickers hardness is assumed to be greater than 45 GPa, thus, all the Si_2N_2O phases are not superhard compounds. The empirical G–H_v, E–H_v relationships and Gao *et al.*'s method can best estimate the microhardness values of the Si_2N_2O polymorphs.

Table 4. Vickers hardness values calculated by Gao *et al.*'s, Miao *et al.*'s, and Jiang *et al.*'s methods, where d^μ is the bond length (Å), n^μ the number of μ-type bond, N_e^μ the valence electron density of a μ-type bond (electrons/Å^3), H_e^μ the hardness of a μ-type bond, and H_v the Vickers hardness of the crystal structure (GPa).

Species	Bond type	d^μ	n^μ	N_e^μ	H_e^μ	H_v (Gao)	H_v (Miao)	H_v (Jiang)	H_v (expt.)
Orthorhombic Si_2N_2O	Si–O	1.6322	4	0.6055	37.33	28.90	15.18	$H_v^{B/10.38} = 15.60$ $H_v^{G/5.68} = 13.82$ $H_v^{E/16.48} = 14.29$	19[11]
	Si–N	1.7344	12	0.3364	26.54				
Tetragonal Si_2N_2O	Si–O	1.7756	24	0.7341	34.06	31.52	44.07	$H_v^{B/10.38} = 26.89$ $H_v^{G/5.68} = 31.76$ $H_v^{E/16.48} = 31.18$	
	Si–N	1.7404	16	0.6578	41.14				
	Si–N	1.8675	48	0.4649	27.37				
Alternative spinel Si_2N_2O	Si–O	1.7941	6	0.7283	33.01	28.95	43.99	$H_v^{B/10.38} = 22.59$ $H_v^{G/5.68} = 29.41$ $H_v^{E/16.48} = 28.28$	
	Si–O	1.8072	18	0.7125	31.95				
	Si–N	1.8601	8	0.4697	27.83				
	Si–N	1.8742	16	0.4592	26.90				
	Si–N	1.8742	8	0.4592	26.90				
	Si–N	1.8517	8	0.4761	28.40				
	Si–N	1.8443	16	0.4819	28.92				
	Si–N	1.8608	8	0.4692	27.79				
α-Al_2O_3-type Si_2N_2O	Si–O	1.9356	16	0.5953	23.87	29.53	38.30	$H_v^{B/10.38} = 27.62$ $H_v^{G/5.68} = 29.72$ $H_v^{E/16.48} = 29.72$	
	Si–O	1.9319	8	0.5987	24.08				
	Si–N	1.8586	16	0.5947	32.64				
	Si–N	1.8556	16	0.5977	32.88				
	Si–N	1.8560	16	0.5973	32.85				
β-Si_3N_4[39]	Si–N	1.715	14	0.453	33.3	33.3		$H_v^{B/10.38} = 24.80$[39] $H_v^{G/5.68} = 21.34$[39]	30±2[40]
γ-Si_3N_4[39]	Si(4)–N	1.750	32	0.74	43.88	33.3		$H_v^{B/10.38} = 30.24$[39] $H_v^{B/10.38} = 29.67$[41] $H_v^{G/5.68} = 48.05$[39] $H_v^{G/5.68} = 44.37$[41]	30[42], 35[43]
	Si(8)–N	1.856	96	0.529	30.34				

4. Conclusions

Some fundamental ground state properties of Si_2N_2O structures are studied using first principles calculations, i.e., electric structures, elastic constants, mechanical moduli, and Vickers hardness. The full set elastic constants are calculated using the stress–strain method in the Voigt–Reuss–Hill approximation. The mechanical moduli are also discussed. The calculated mechanical moduli, i.e., bulk modulus, shear modulus, and Young's modulus, indicate that tetragonal Si_2N_2O are superior to those of the other three phases. Orthorhombic Si_2N_2O has a relatively small mechanical modulus. The Vickers hardness value of Si_2N_2O is estimated by three semi-empirical methods. The results imply that tetragonal Si_2N_2O is the hardest phase in the four Si_2N_2O structures. The Vickers hardness values of the two monoclinic Si_2N_2O phases are close to each other. The hardness value of tetragonal Si_2N_2O is 31.52 GPa which is close to values of β-Si_3N_4 and γ-Si_3N_4.

Acknowledgment

We thank the Institute of Solid State Physics &, the School of Physics and the Electronic Engineering Department of Sichuan Normal University for the

computational support.

References

[1] Buchanan D A 1999 *IBM J. Res. Develop.* **43** 245

[2] Roucka R, Tolle J, Chizmeshya A V G, Crozier P A, Poweleit C D, Smith D J, Tsong I S T and Kouvetakis J 2002 *Phys. Rev. Lett.* **88** 206102

[3] Roucka R, Tolle J, Crozier P A, Smith D J, Tsong I S T and Kouvetakis J 2001 *Appl. Phys. Lett.* **79** 2080

[4] Kaufman L 1979 *Calphad* **3** 275

[5] Ohashi M, Kanzaki S and Tabata H 1991 *J. Am. Ceram. Soc.* **74** 109

[6] Ohashi M, Kanzaki S and Tabata H 1991 *J. Mater. Sci.* **26** 2608

[7] Brosset C and Idrestedt I 1964 *Nature* **201** 1211

[8] Srinivasa S R, Cartz L, Jorgensen J D, Worlton T G, Beyerlein R A and Billy M 1977 *J. Appl. Cryst.* **10** 167

[9] Sjoeberg J, Helgesson G and Idrestedt I 1991 *Acta Cryst.* C **47** 2438

[10] Radwan M, Kashiwagi T and Miyamoto Y 2003 *J. Eur. Ceram. Soc.* **23** 2337

[11] Xiong LT, Cao M S and Hou Z L 2009 *Chin. Phys. Lett.* **26** 076201

[12] Poon C O, Wong F L, Tong S W, Zhang R Q, Lee C S and Lee S T 2003 *Appl. Phys. Lett.* **83** 1038

[13] Eldada L 2004 *Rev. Sci. Instrum.* **75** 575

[14] Li J S and He S L 2005 *Opt. Commun.* **254** 236

[15] Mirgorodsky A P, Baraton M I and Quintard P 1989 *J. Phys: Condens. Matter* **1** 10053

[16] Yao H Z, Ouyang L Z and Ching W Y 2007 *J. Am. Ceram. Soc.* **90** 3194

[17] Xu Y N and Ching W Y 1995 *Phys. Rev.* B **51** 17379

[18] Ohashi M, Nakamura K, Hirao K, Toriyama M and Kanzaki S 1997 *Ceram. International* **23** 27

[19] Kroll P and Milko M Z 2003 *Anorg. Allg. Chem.* **629** 1737

[20] Sekine T, He H L, Kobayashi T and Shibata K 2006 *American Mineralogist* **91** 463

[21] Haines J and Santoro M 2008 *Phys. Rev.* B **77** 144206

[22] Liu B, Wang J Y, Li F Z, Tong Q F and Zhou Y C 2009 *J. Phys. Chem. Solids* **70** 982

[23] Zhang T, Wu M Q, Zhang S R, Chen S, He M, Wang J M, Zhang D H, He F M and Li Z P 2011 *J. Alloys Compd.* **509** 1739

[24] Chen H C and Yang L J 2011 *Acta Phys. Sin.* **60** 014207 (in Chinese)

[25] Ru Q, Hu S J and Zhao L Z 2011 *Acta Phys. Sin.* **60** 036301 (in Chinese)

[26] Yang T X, Cheng Q, Xu H B and Wang Y X 2010 *Acta Phys. Sin.* **59** 4919 (in Chinese)

[27] Xu H B and Wang Y X 2009 *Acta Phys. Sin.* **58** 5645 (in Chinese)

[28] Gou H Y, Gao F M, Zhang J W and Li Z P 2011 *Chin. Phys.* B **20** 016201

[29] Perdew J P, Ruzsinszky A, Csonka G I, Vydrov O A, Scuseria G E, Constantin L A, Zhou X L and Burke K 2008 *Phys. Rev. Lett.* **100** 136406

[30] Laasonen K, Pasquarello A, Car R, Lee C and Vanderbilt D 1993 *Phys. Rev.* B **47** 10142

[31] Ching W Y 2004 *J. Am. Ceram. Soc.* **87** 1996

[32] Wu Z J, Zhao E J, Xiang H P, Hao X F, Liu X J and Meng J 2007 *Phys. Rev.* B **76** 054115

[33] Ravindran P, Fast L, Korzhavyi P A, Johansson B, Wills J and Eriksson O 1998 *J. Appl. Phys.* **84** 4891

[34] Xiao B, Feng J, Zhou C T, Jiang Y H and Zhou R 2011 *J. Appl. Phys.* **109** 023507

[35] Boch P and Glandus J C 1979 *J. Mater. Sci.* **14** 379

[36] Jiang X, Zhao J J and Jiang X 2011 *Compd. Mater. Sci.* **50** 2287

[37] Miao N H, Sa B S, Zhou J and Sun Z M 2011 *Compd. Mater. Sci.* **50** 1559

[38] Gao F M, He J L, Wu E D, Liu S M, Yu D L, Li D C, Zhang S Y and Tian Y J 2003 *Phys. Rev. Lett.* **91** 015502

[39] He J L, Guo L C, Yu D L, Liu R P and Tian Y J 2004 *Appl. Phys. Lett.* **85** 5571

[40] Andrievski R A 2001 *Int. J. Refract. Met. Hard Mater.* **19** 447

[41] Kocer C, Hirosaki N and Ogata S 2003 *Phys. Rev.* B **67** 035210

[42] Soignard E, Somayazulu M, Dong J, Sankey O F and McMillan P F 2001 *J. Phys.: Condens. Matter* **13** 557

[43] Jiang J Z, Kragh F, Frost D J, Ståhl K and Lindelov H 2001 *J. Phys.: Condens. Matter* **13** L515